Available online at www.sciencedirect.com
ScienceDirect
Journal of Power Sources 176 (2008) 435–443
JOURNAL OF POWER SOURCES
www.elsevier.com/locate/jpowsour

The effect of ammonium ions on oxygen reduction and hydrogen peroxide formation on polycrystalline Pt electrodes

Rune Halseid *, Martin Heinen, Zenonas Jusys, R. Jürgen Behm *

Institute of Surface Chemistry and Catalysis, Ulm University, D-89069 Ulm, Germany

Available online 2 September 2007

Abstract

The influence of ammonium ions on the activity and selectivity of the electrocatalytic oxygen reduction reaction (ORR) on polycrystalline Pt was investigated in model studies under continuous mass transport, both in sulfuric and perchloric acid solutions. Ammonium was found to increase the yield of hydrogen peroxide, particularly in sulfuric acid, but also in perchloric acid solutions, and also at higher potentials (0.80–0.90 V_{RHE}) typical for fuel cell cathode operation, which may severely impair the long-term stability of membranes and electrodes in fuel cells exposed to fuel gases and/or air containing ammonia. Adsorbed species, assigned to ammonia and nitric oxide, were identified on a Pt film electrode using *in situ* FTIR spectroscopy. Adsorbed nitric oxide could only be observed in perchloric acid solutions. The higher coverage of adsorbed ammonia in sulfuric acid solution is attributed to a stabilization by coadsorbed (bi-)sulfate species; the higher total coverage in this electrolyte can explain the larger effect of ammonium ions on the ORR activity and selectivity in sulfuric compared to perchloric acid solution.

Keywords: Oxygen reduction reaction; Activity; Selectivity; Hydrogen peroxide formation; NH_3 effects; Platinum

1. Introduction

Recently, there has been a growing interest in ammonia poisoning of polymer electrolyte fuel cells (PEFC) [1–3]. Ammonia may be present in the hydrogen fuel for several reasons: (i) due to formation of NH_3 in reformers operated with air [4], (ii) due to metal hydride catalyzed formation of NH_3 from traces of N_2 in the H_2 used to re-fuel these storages [5], or (iii) due to residual NH_3 in the fuel gas, if NH_3 is used as a hydrogen carrier. Ammonia may also enter the fuel cell via ambient air fed to the cathode. In the end, it is probably less important whether the ammonia enters the fuel cell on the anode or cathode side, as the diffusion of ammonium from one side to the other is fast. For instance, for a typical membrane thickness (l) of 10–100 μm and a diffusivity of ammonium ions of 10^{-10} m^2 s^{-1}, the estimated characteristic time constant for diffusion is $\tau_{diff} \sim l^2/D_{NH_4^+} = 1\text{–}100\,s$ [3].

Ammonia may affect the PEFC performance in different ways: (i) by reduction of the ionic conductivity of the membrane, which in its ammonium form is by a factor of four lower than in the protonated form [2,3,6], (ii) by poisoning of the cathode catalyst in the oxygen reduction reaction (ORR) [7], and (iii) by similar effects on the anode catalyst, in the hydrogen oxidation reaction (HOR) [3]. Recently, fuel cell measurements have shown that the reduced membrane conductivity is not the major reason for performance losses induced by ammonia [2,3]. The effect of ammonia on the HOR was found to be small at current densities below 0.5 A cm^{-2}, but to increase with higher currents, and the current density did not exceed 1 A cm^{-2} in the presence of ammonia [3]. The reason for this current limit was not established; model studies in liquid electrolyte are difficult to compare as the solubility of hydrogen and thus the limiting current is low. However, it is clear that the effect of ammonia in the fuel gas on the ORR is of large importance to understand the performance loss in fuel cells exposed to ammonia.

A significant influence of ammonium ions on the ORR has previously been reported in model studies in aqueous sulfuric acid solution [7]. (In the following, we will refer to ammonium ions as ammonium.) The exchange current compared to that in neat acid was 90% lower on pre-reduced Pt (positive-going scan in potentiodynamic measurements) and 75% lower on pre-oxidized Pt (negative-going scan in potentiodynamic measurements), when ammonium was present. The Tafel slopes were also affected, most noticeable at low current densities on

* Corresponding authors.
E-mail addresses: halseid@hotmail.com (R. Halseid), juergen.behm@uni-ulm.de (R. Jürgen Behm).

0378-7753/$ – see front matter © 2007 Elsevier B.V. All rights reserved.
doi:10.1016/j.jpowsour.2007.08.067

pre-reduced Pt and at high current densities on pre-oxidized Pt. Finally, it is also known from studies of phosphoric acid fuel cells that the ammonia-induced performance loss mainly occurs at the cathode [8]. In addition to the activity, the presence of ammonia in the feed may also alter the selectivity of the ORR, to the (desired) four-electron pathway to H_2O or to the (undesired) two-electron pathway to H_2O_2, which would be highly relevant for technical applications because of the possible negative effect of H_2O_2 on the long-term durability of the PEFC membrane and electrodes [9], although the hypothesis that H_2O_2 is the major factor contributing to membrane degradation, was questioned recently [10].

Extending recent work, where the authors reported on the influence of ammonium on the ORR activity in sulfuric solutions [7], we here present new data on the effect of ammonium on the ORR activity and selectivity on a polycrystalline Pt electrode in sulfuric and perchloric acid electrolytes, both under potentiodynamic and potentiostatic conditions. Due to the weak specific adsorption of perchlorate on Pt, the latter is a better representation of the actual conditions found in a PEFC. The experiments were performed in a dual-electrode thin-layer flow cell, which allows measurements under controlled, continuous electrolyte flow [11]. Furthermore, we present complementary *in situ* FTIR spectro-electrochemical data recorded on polycrystalline Pt film electrodes in O_2-saturated electrolytes containing ammonium, to identify the adsorbed species and thus obtain information on their impact on the ORR activity and selectivity.

2. Experimental

2.1. Bulk oxygen reduction with ammonium-containing electrolytes

The dual-electrode thin-layer flow cell used in these experiments has been described in more detail elsewhere [11]. The generator electrode, a 9 mm diameter polycrystalline Pt cylinder (MaTecK, 99.95% purity), was mounted into the flow cell, pressing against an approximately 50 μm thick spacer. This exposes 0.28 cm^2 Pt surface to the thin-layer electrolyte volume. The electrolyte entered the center of the first compartment and flowed in a radial pattern over the generator electrode towards the edge and into the second compartment. There the electrolyte flowed over the collector electrode, a polycrystalline 1.13 cm^2 Pt foil, held at a fixed potential (1.10 V), where electroactive intermediate species, in our case H_2O_2, were detected. The electrolyte flow was approximately 5 μl s^{-1}, resulting in a delay time between the generator and collector of about 2 s.

A Pine AFRDE5 bipotentiostat was used for potential control, and data were logged using the LabVIEW software (National Instruments). A reversible hydrogen electrode (RHE) was used as reference electrode (RE) and was connected via a PTFE capillary to the cell outlet; all potentials are quoted versus that of the RHE reference. Two Pt counter electrodes (CEs) interconnected by an external resistor were used.

The potential of the generator electrode was swept at 10 mV s^{-1} in the potentiodynamic measurements. Prior to the measurements, the electrodes were cleaned electrochemically by cycling the potential between ~0 and 1.35 V at sweep rates of 100–200 mV s^{-1}.

The collection efficiency η_{coll} of the collector was determined by generating H_2 at the generator, 1–45 μA, then oxidizing this at the collector, biasing the collector at 0.40 V. The collection efficiency, η_{coll}, increased by a few percent with generator current; in the analysis of the ORR data a constant collection efficiency of 80%, about four times higher than that attainable in conventional RRDE experimental setup [12], was used. The collector data were filtered digitally with the filtfilt function in Matlab®. The relative yield of H_2O_2 from the ORR, $y_{H_2O_2}$, was calculated from the following equation [12]:

$$y_{H_2O_2} = \frac{i_{coll}/2\eta_{coll}}{i_{gen}/4 + i_{coll}/2\eta_{coll}} \quad (1)$$

where i_{gen} and i_{coll} denote the currents on the generator and collector, respectively.

The real surface area of the electrodes was determined from hydrogen underpotential deposition (H_{upd}), assuming a H_{upd} monolayer charge of 210 μC cm^{-2} and that a H_{upd} coverage of 77% of a full monolayer is reached in the potential range used for charge integration [13]. The real surface area of the electrode determined in sulfuric acid was used also when evaluating data from perchloric acid.

The kinetic current, i_k, was determined from:

$$i_k = i\frac{i_d}{i_d - i} \quad (2)$$

where i is the measured current and i_d is the mass transfer limited current observed at low potentials in the potential scans. To determine the Tafel parameters, the current recorded in neat acid in the absence of O_2 was subtracted from the ORR data recorded in O_2-saturated electrolyte to eliminate the current related to surface processes on Pt such as formation/removal of Pt oxides from the ORR data. No corrections for ohmic effects were made.

2.2. Ammonium adsorption/stripping experiments

After electrochemical pre-cleaning, the WE was exposed to O_2-saturated acid containing ammonium, and the ORR transients at constant potentials (0.50, 0.60, 0.70, 0.75 and 0.80 V) were followed for 10 min before neat, O_2-saturated acid was introduced again. The relaxation transient, recorded in neat, O_2-saturated acid solution while keeping the potential constant, was then followed for another 5 min. Simultaneously, the H_2O_2 oxidation current was measured by the collector.

Stripping of adsorbates formed on the electrode, after interaction with O_2-saturated, ammonium-containing solution at a fixed potential for 4 min, was performed in neat, O_2-saturated acid.

2.3. ATR–FTIRS measurements

The cell used for the *in situ* FTIR spectroscopy measurements in an attenuated total reflection (ATR) configuration [14,15] is similar to the cell used for generator/collector studies described above. In this case, however, the WE was a thin Pt film formed

by electroless plating of a Pt film (~50 nm) on the flat surface of a hemi-cylindrical silicon prism [16]. The flat surface of the prism was pressed against a spacer so that a thin electrolyte layer was formed, exposing a total geometric Pt area of 1.13 cm^2 to the electrolyte. The real surface area was determined from H_{upd} as described above, yielding a roughness factor of 5.8. The electrode potential was controlled using a Bank Wenking Pos 2 potentiostat, and IR spectra were measured with a Bio-Rad FTS 6000 instrument at 4 cm^{-1} resolution. Spectra were collected every 0.2 s and co-added for 1 or 5 s for potentiostatic adsorption experiments or potentiodynamic experiments, respectively. The IR data are presented as relative absorbance, defined as $A = \log_{10} R_0 - \log_{10} R$, where R is the reflectance in the respective measurement and R_0 is the reflectance in the reference spectrum (typically recorded in neat acidic solution at low electrode potential). In this presentation positive peaks indicate an increased IR absorption, *i.e.*, an increased concentration of the surface species. The absorption data were filtered in the same way as described above for the collector data.

2.4. Chemicals

Ammonium hydroxide (25%), perchloric acid and sulfuric acid (all Suprapur from Merck) were used as received in all experiments and solutions were prepared using high purity water from a Millipore Milli-Q Plus system. 0.50 M solutions of the acids were used with additions of NH_4OH as noted. Solutions were deaerated with Ar (MTI Gase, N6) or saturated with O_2 (MTI Gase, N5.5). All experiments were carried out at room temperature (~22 °C).

3. Results and discussion

3.1. Effect of ammonium on the ORR kinetics

The effect of ammonium on the ORR activity in perchloric acid solution, as measured in potentiodynamic scans in ammonium-free and ammonium-containing O_2-saturated solution, is illustrated in Fig. 1a for pre-reduced (positive-going scan) and pre-oxidized (negative-going scan) Pt. The effect of ammonium is negligible in the potential range of the ORR onset, both in the positive-going and negative-going scan. In the range of higher ORR currents, the presence of ammonium leads to an increased overpotential of between 24 mV (0.1 M NH_4OH) and 63 mV (0.25 M NH_4OH) for pre-reduced Pt at a kinetic current of 0.1 A cm^{-1} and between 38 and 75 mV for pre-oxidized Pt under the same conditions (see Tafel plots in Fig. 2a).

The hydrogen peroxide production and yield increased in the potential region 0.20–0.80 V in the negative-going scans, when ammonium was present in the perchloric acid solution (Fig. 1b and c), but there was no effect of ammonium on the ORR selectivity in the positive-going scan. At very low potentials, below 0.20 V, the H_2O_2 production is significant also in neat acid, as has also been reported previously [12,17,18]. The small reductive current in the positive-going sweep at 0.92 V is an artifact, caused by the use of two CEs. The impact can be minimized by applying a large resistor in the circuit for CE2. The noticeable peak in the H_2O_2 formation rate appearing in ammonium-containing solution in the negative-going scans at 0.90–0.60 V can be explained by the presence of Pt-oxides in neat acid and possible nitric oxides in solutions containing ammonium, which partially block the Pt surface and thus enhance the formation of hydrogen peroxide. This interpretation is based on the findings in previous studies, where it had been observed that adsorbates formed at high potentials are very stable [19,20]. Furthermore, it is known that the formation of H_2O_2 increases when adsorbates are present on the Pt surface [12,17,18,21,22]. Hence, the formation of ammonium-related adsorbates at high potentials can explain why more H_2O_2 is formed in the potential range 0.9–0.75 V and also that its formation extends to lower potentials than in neat acid (the onset of H_2O_2 is at about 0.90 V in all solutions in Fig. 1).

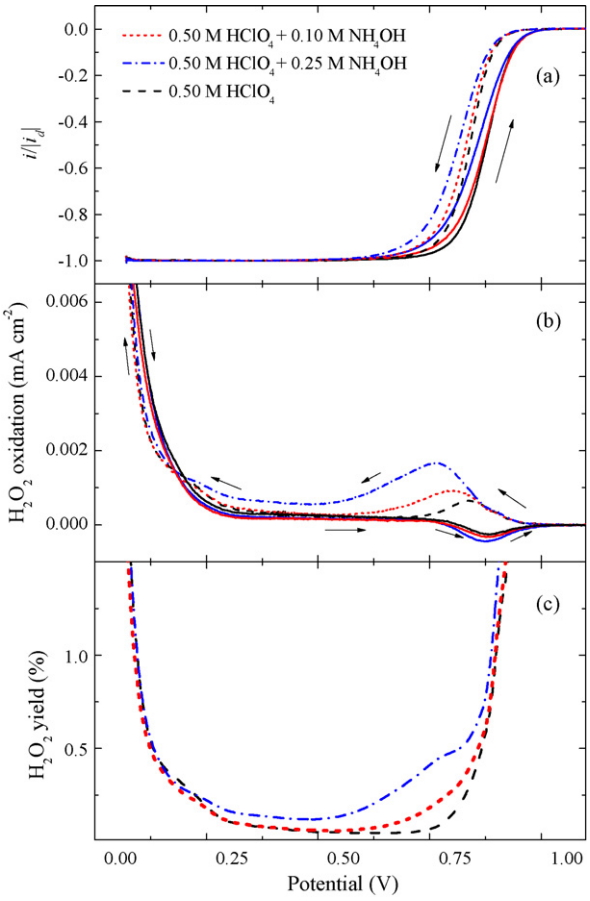

Fig. 1. Normalized ORR current (i/i_d) on a polycrystalline Pt electrode (a), hydrogen peroxide oxidation current at the polycrystalline Pt collector (b) due to H_2O_2 formed at the working electrode in ammonium-containing perchloric acid solutions, and the relative yield of H_2O_2 in the ORR in the negative-going scan (c). Broken lines represent negative-going scans, solid lines positive-going scans (E_{coll} = 1.10 V, η_{coll} = 80%, 10 mV s^{-1}, electrolyte as indicated in the figure).

Tafel plots of the ORR kinetic currents in perchloric acid in the absence and presence of ammonium, derived from the potentiodynamic data in Fig. 1, are depicted in Fig. 2. Similar Tafel data obtained from RDE measurements in sulfuric acid have been reported previously in Ref. [7]. In perchloric acid, the effect of ammonium on the ORR process on polycrys-

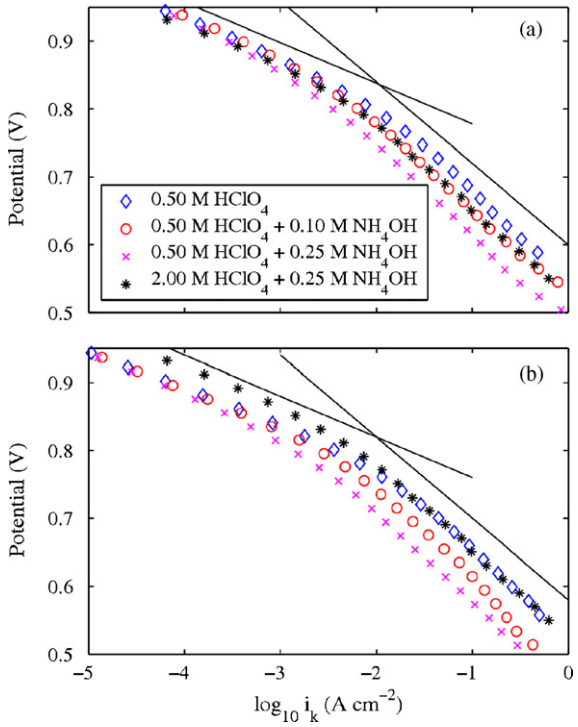

Fig. 2. Tafel plots of the kinetic currents, i_k, for O_2 reduction during potentiodynamic scans in (a) positive-going and (b) negative-going scan on polycrystalline Pt. The oxidation rate was measured in a flow cell (scan rate 10 mV s^{-1}, electrolyte as indicated in the figure). The measurements were initiated at low potentials and reversed at 1.15 V. Tafel slopes corresponding to −60 and −120 mV dec^{-1} are shown as solid lines for comparison.

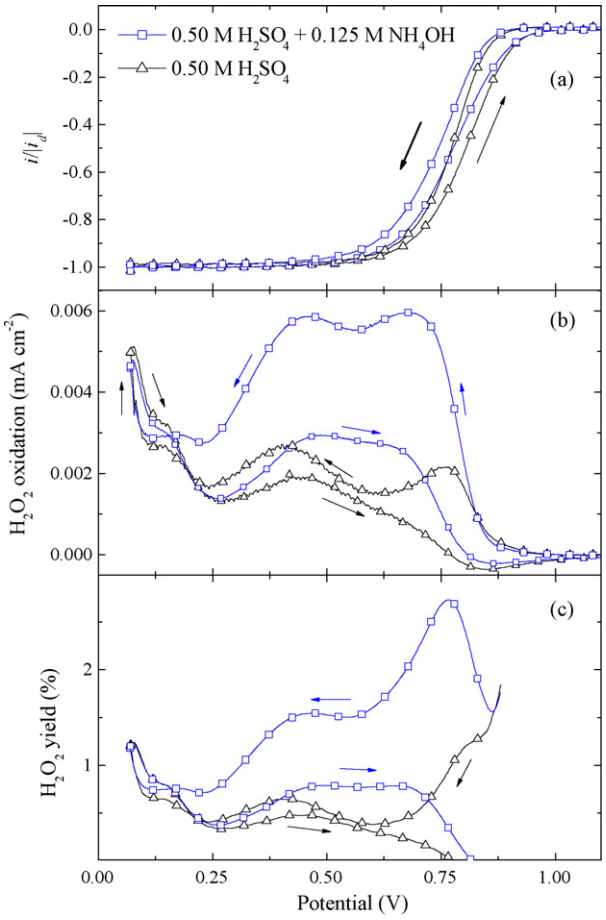

Fig. 3. Normalized ORR current (a), hydrogen peroxide oxidation formation (b) and relative yield of H_2O_2 in the ORR (c) on polycrystalline Pt in O_2-saturated sulfuric acid solutions (E_{coll} = 1.10 V, η_{coll} = 80%, 10 mV s^{-1}, electrolyte as indicated in the figure). Scan directions are indicated with arrows.

talline Pt was relatively small. Neither the Tafel slopes nor the exchange current density were significantly affected by addition of ammonium. However, the transition from the low-slope region to the high-slope region occurred at lower current densities when ammonium was present in the solution. In sulfuric acid, the ammonium-induced effects were more significant; Tafel slopes, exchange current density as well as the onset of the high-slope region were affected by the presence of ammonium [7]. Furthermore, the kinetic currents in perchloric acid are higher than in sulfuric acid. A similar anion effect on the ORR kinetics has also been reported in [12,17,23], it was ascribed to the stronger specific adsorption of (bi-)sulfate on Pt, whereas perchlorate adsorbs only weakly.

Similar experiments as presented in Fig. 1 were performed also in sulfuric acid solution (Fig. 3). In that case, the effect of ammonium on the ORR activity and on the H_2O_2 formation, *i.e.*, on the ORR selectivity, was more severe than in perchloric acid. The H_2O_2 yield was as high as 2–3% at potentials, where PEFC cathodes are typically operated (0.60–0.90 V). H_2O_2 formation is assumed to be more pronounced in sulfuric acid than in perchloric acid because (bi-)sulfate adsorbs specifically on the Pt surface, in addition to the oxide layer formed, which results in more extensive blocking of the Pt surface than in the case of perchloric acid (see also Section 3.4). This in turn is known to lead to higher H_2O_2 yields (see Fig. 3c)), due to a decrease in the number of neighboring Pt sites required for O_2 adsorption/dissociation and reduction to water.

In addition to the different adsorption strength of the anions, also the pH of the solutions, which significantly increased upon addition of ammonium hydroxide, may lead to modifications in the ORR characteristics. To decrease the pH, a solution of 2.00 M $HClO_4$ + 0.25 M NH_4OH was used, and the related data are also shown in Fig. 2. They demonstrate that the effect of ammonium addition on the ORR in perchloric acid is indeed pH dependent.

3.2. ORR transients in ammonium-containing electrolyte

In order to more closely simulate the situation in a fuel cell, constant potential measurements were performed as well, ORR current transients were recorded upon changing from ammonium-free to ammonium-containing sulfuric acid electrolyte at different potentials between 0.50 and 0.80 V, and the time evolution of the hydrogen peroxide yield are shown in Fig. 4. The Pt surface was pre-reduced, *i.e.*, the preceding potential sweep was stopped in the positive-going direction before the transients were initiated. When the electrode was exposed to ammonium-containing electrolyte at $t = 0$, the ORR current decreased rapidly. This current decay was much more severe for potentials in the range 0.70–0.80 V than below 0.70 V. The dif-

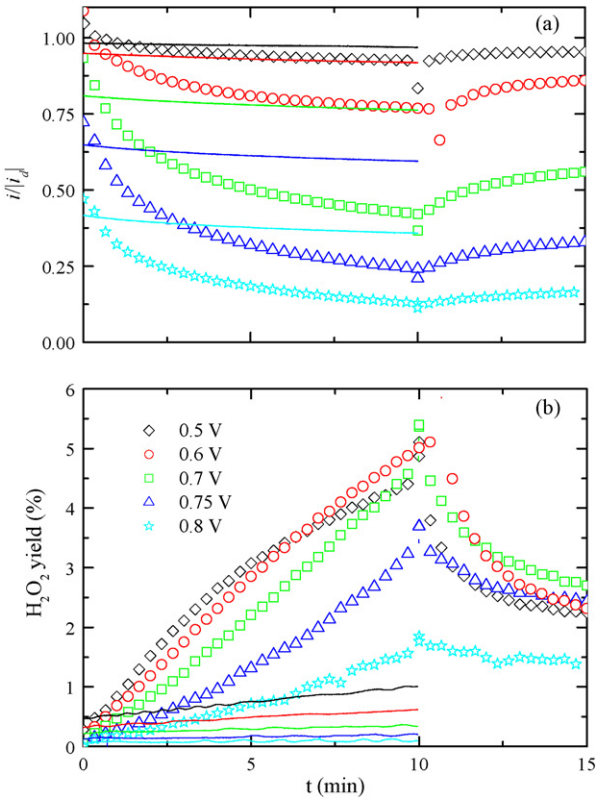

Fig. 4. ORR transients observed when changing from a flow of O_2-saturated, neat 0.50 M H_2SO_4 to O_2-saturated 0.50 M H_2SO_4 + 0.125 M NH_4OH through the cell for 10 min, followed by 5 min of O_2-saturated, neat 0.50 M H_2SO_4 at different electrode potentials. (a) Normalized ORR current, *i.e.*, ORR current relative to the mass transfer limited current in the same solution and (b) H_2O_2 yield. The straight lines included in both plots were measured in O_2-saturated neat acid at the same potentials and are shown for comparison. All measurements were performed on pre-reduced Pt, *i.e.*, the electrochemical pre-cleaning scan in neat, O_2-saturated acid was stopped at the desired potential in the positive-going scan before O_2-saturated solution containing ammonium was admitted to the cell.

ference results from the fact that at 0.7–0.8 V the ORR is largely kinetically controlled, while at lower potentials also the mass transfer limitations influence the attainable ORR current. The ORR currents in ammonium-containing electrolyte, shown as normalized ORR current i/i_d, were initially slightly higher than those observed in neat acid. This is due to an experimental artifact, resulting from normalizing the current by the i_d measured in ammonium-containing electrolyte, and the finite time required for exchanging the ammonium-free by ammonium-containing electrolyte. The limiting ORR current in neat acid is higher than in the presence of ammonium due to salting-out effects in the latter electrolyte [7], *i.e.*, the solubility of O_2 decreases with increasing ionic strength of the solution. When switching from ammonium containing, O_2-saturated acid to O_2-saturated neat acid, the ORR activity of the electrode increased, but did not recover to the same level as prior to ammonium exposure. At the highest potential, 0.80 V, the recovery of the ORR activity was marginal. The formation of H_2O_2 also increased significantly during the adsorption transients and did not level off within the time allowed for adsorption in this study (10 min). Further, the H_2O_2 formation rate decreased when changing the electrolyte to neat acid. But also then, the H_2O_2 formation rate was significantly higher than before the cell was exposed to ammonium. These data strongly suggest that both ORR activity and selectivity are severely influenced by irreversibly adsorbed ammonium residues, whose coverage passes through a maximum at 0.60–0.70 V. These issues were studied in more detail at different adsorption potentials, as will be presented and discussed in the following section.

A second important observation from these data is the rather low rate of the ammonium-induced poisoning process. Even after 10 min in 0.125 M NH_4OH containing electrolyte, steady state had not been reached; in particular not for the H_2O_2 formation rate (Fig. 4). This agrees well with previous observations in potentiodynamic ORR experiments, where the applied scan rate had a significant effect on the ORR polarization curve in sulfuric acid containing ammonium [24]. This kinetic aspect is of course also of practical importance for fuel cells being operated for long periods of time. In PEFC testing, it has been noted that the poisoning caused by ammonia is rather gradual and takes a long time to approach a steady state [1–3]. This is partly due to the low content of ammonia in the gas phase, so that the ammonium concentration in the fuel cell membrane, which has a high solubility for ammonium, increased only slowly. To another part, it is caused by the slow uptake of ammonia and formation of ammonium-related adsorbates on the cathode catalyst, as indicated by the present data.

3.3. *Effect of ammonium pre-adsorption on the ORR*

The effect of pre-adsorbed ammonium on the ORR activity and selectivity on polycrystalline Pt in sulfuric acid solution was evaluated in a series of slow potential scans (10 mV s^{-1}) in O_2-saturated neat acid solution, recorded after 4 min ammonium adsorption at different adsorption potentials (Fig. 5).

Exposure of the WE to O_2-saturated, ammonium-containing electrolytes at 0.40 V and lower had no significant effect on the ORR activity in the subsequent potential scan. In contrast, the production of H_2O_2, *i.e.*, the selectivity of the ORR, was modified much more severely, yielding an increasing fraction of incomplete O_2 reduction to H_2O_2. For adsorption potentials between 0.50 and 0.75 V, we find a significant decrease of the ORR rate (Fig. 5a), and also increased formation of H_2O_2 (Fig. 5b). Finally, above 0.75 V, there was no further effect on the ORR. The formation rate for H_2O_2 on the adsorbate covered electrode, in the subsequent potential scan, reached a maximum upon adsorption at potentials in the range of 0.65–0.70 V.

The effects on H_2O_2 formation were significant also in the subsequent negative-going sweep, after scan reversal at 1.15 V (Fig. 5d), indicating that not all of the ammonium adsorbates were removed oxidatively. In contrast, the ORR currents were only slightly affected in the negative-going sweep (Fig. 5c). In the following positive-going sweep (*i.e.*, after 1.5 sweeps), we found no measurable effects of the initial adsorption potential on the ORR activity and H_2O_2 formation (data not shown here), and activity and selectivity are as shown in Fig. 5b in neat acid. Furthermore, if the sweep was initially negative-going, no difference compared to neat acid could be observed in the ORR

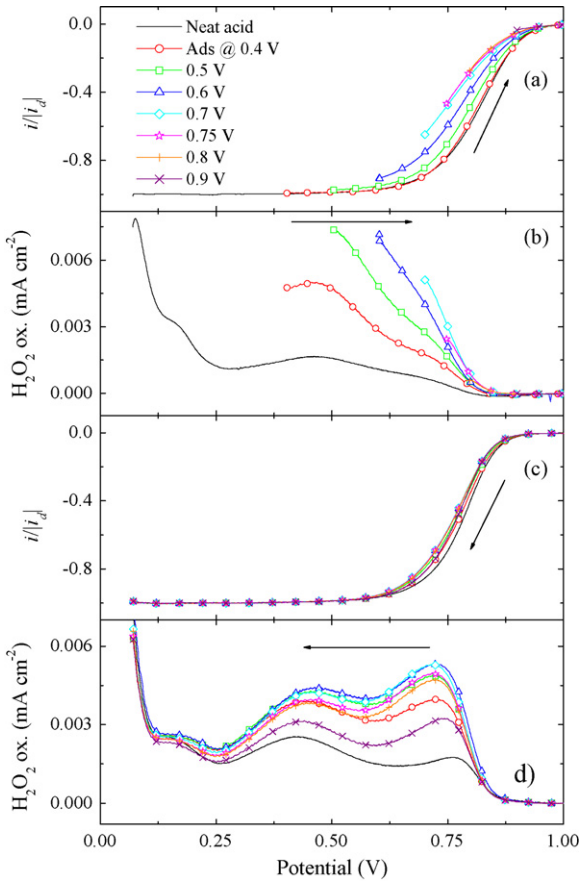

Fig. 5. Positive-going (a and b) and negative-going (c and d) scans after ammonium adsorption from a solution containing 0.125 M NH_4OH in 0.50 M H_2SO_4 for 4 min at different adsorption potentials (potentials see figure). (a) and (b) show the normalized ORR current during the positive-going scans and the corresponding H_2O_2 signals from the collector (E_{coll} = 1.10 V, collection efficiency ca. 80%); (c) presents the normalized ORR current recorded during the following negative-going scan and (d) the corresponding H_2O_2 signal (polycrystalline Pt, 10 mV s^{-1}, room temperature).

activity and selectivity in the subsequent positive-going scan, after the initially negative-going sweep to low potentials. In combination, these results imply that the adsorbed species causing the decay in ORR activity and in particular in selectivity were largely removed reductively at low potentials. This is discussed further in the next sections.

The formation of hydrogen peroxide is promoted by the presence of ammonium in perchloric acid (Fig. 1) and, even more pronounced, in sulfuric acid solution (Figs. 3–5). It also depends strongly on the adsorption time and potential (see Figs. 4 and 5). While the ORR activity is hardly affected by ammonium adsorption at potentials below 0.50 V, where the mass transport limitations become important, the ORR selectivity is still sensitive to that. Nevertheless, the highest decay in selectivity during the adsorption transients (Fig. 4) occurs in the same adsorption potential region in which also the decay in ORR activity is strongest, at about 0.60–0.70 V. The fact, that changes in the ORR selectivity commence at lower potentials than changes in the ORR activity, could indicate that there are either different species involved, if we presume that these effects are due to adsorbed species, or, alternatively, that the ORR selectivity, is affected at lower surface coverages of the adsorbed species than the ORR activity. The latter could occur, *e.g.*, if the mass transfer of O_2 to the electrode is too low to observe effects on the ORR activity at these lower potentials.

3.4. *In situ* ATR–FTIRS identification of adsorbed intermediates

To identify adsorbed ammonium residues and to evaluate their impact on the ORR activity, *in situ* spectro-electrochemical FTIRS measurements were conducted on a Pt film electrode in a thin-layer flow cell [15]. The formation of ammonium-related adsorbates was monitored during exposure to ammonium-containing, O_2-saturated solutions at a constant potential of 0.60 V. Changing to ammonium-containing solution, new absorption bands appeared in the IR spectra (see set of IR spectra in Fig. 6). A band at 1280 cm^{-1} was observed in both sulfuric and perchloric acid electrolytes, as well as a band at about 1460 cm^{-1}. The former has previously been attributed to the symmetric deformation ("umbrella") mode of ammonia adsorbed on Pt(1 1 1) via the lone pair orbital [25], whereas the latter has been assigned to absorption of bulk-like ammonium, via the δ_{HNH} bending mode [26,27]. ATR measurements are little sensitive to bulk species, and it is therefore likely that the bulk-like ammonium band observed at 1460 cm^{-1} is due to ammonium ions adsorbed in the outer Helmholtz plane (OHP). The absorption frequency for ammonium in the OHP is expected to be very close to that of ammonium in the bulk solution. Both peaks were observed also upon adsorption at potentials of 0.20, 0.40 and 0.75 V, but not at 1.10 V. The 1280 cm^{-1} peak is observed upon adsorption in both sulfuric and perchloric acid solutions, but stronger in sulfuric acid solution.

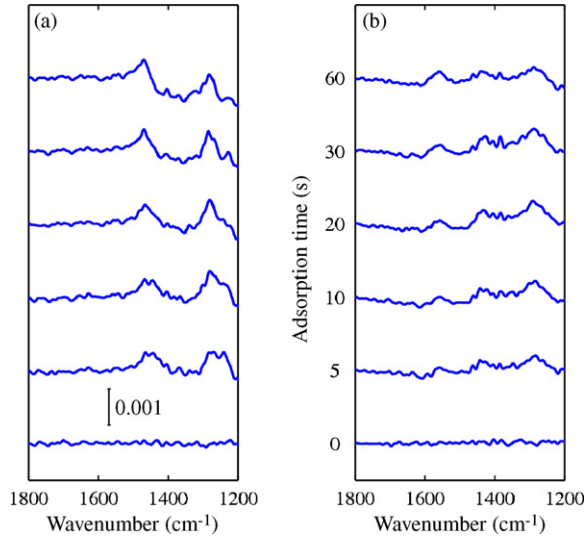

Fig. 6. Selected IR spectra from a set recorded during exposure of the Pt film electrode to ammonium-containing solution at 0.60 V, after switching from neat acid (O_2-free) to O_2-saturated solutions: (a) to 0.50 M H_2SO_4 + 0.25 M NH_4OH and (b) to 0.50 M $HClO_4$ + 0.25 M NH_4OH solution. The reference spectrum was recorded in neat, O_2-free acid at 0.60 V, just before the ammonium-containing electrolyte was admitted to the cell (adsorption times see figure).

In sulfuric acid solution (Fig. 6a), there also seemed to be a shoulder to the 1280 cm^{-1} peak at 1240 cm^{-1}, probably due to increased adsorption of (bi-)sulfate on Pt in the presence of ammonium. This agrees well with previous findings by Shingaya et al. [25], who found two bands at the same frequencies in their study of the interaction of 0.01–0.1 M ammonium in 0.1 M sulfuric acid solution with Pt(1 1 1) and assigned these to coadsorbed ammonia and (bi-)sulfate species.

There is a further weak band at ~1560 cm^{-1} in perchloric acid containing ammonium that is not seen in sulfuric acid. This band was not detected at other adsorption potentials used (0.20, 0.40, 0.75 and 1.10 V, spectra not shown). Absorption bands in this region have been reported for different NO species, depending on the adsorbate coverage, potential and surface orientation [28,29]. Absorption frequencies in the range 1580–1680 were assigned to ν_{N-O} of multifold coordinated NO on Pt(1 1 1) and Pt(1 0 0), with pronounced Stark-tuning slopes in the range of 42–95 cm^{-1} V^{-1} [28]. Momoi et al. reported absorption features at 1520 and 1543 cm^{-1} on Pt(1 1 1) at potentials above 0.95 V, which they attributed to the stretch vibrations $\nu_{N=O}$ of μ-NO_2 and nitrite ONO species in deuterated $DClO_4$ and in HF solutions [30]. The absorption band is also close to the absorption band for water at 1630 cm^{-1}, which makes it more difficult to resolve these small effects. We tentatively assign the band at 1560 cm^{-1} to adsorbed NO species, but there are other possible species reported in the literature [28–30]. Considering that this adsorbed NO species is only seen in perchloric acid, where also H_2O_2 formation is weaker than in sulfuric acid, this species cannot be responsible for the increased H_2O_2 formation in the presence of ammonium.

IR spectra were also recorded during cyclic sweeps in neat, O_2- and ammonium-free acid solution after the adsorption experiments, *i.e.*, during adsorbate stripping. In addition to the spectra recorded in the first cycle (adsorption potential → 1.3 → 0.06 V, Fig. 7, thick lines), we also present spectra recorded in the following sweep (0.06 → 1.30 → 0.06 V, Fig. 7, thin lines) for comparison. Selected spectra from the set recorded after adsorption at 0.60 V are shown in Fig. 7. A band at 1280 cm^{-1} ("umbrella" mode of co-adsorbed ammonia), which is marked (i) and (iii) in Fig. 7a and b, respectively, was found after adsorption in sulfuric acid (Fig. 7a) as well as after adsorption in perchloric acid (Fig. 7b), similar to the observations in ammonium-containing electrolytes (see Fig. 6). Although this band appears in both electrolytes, it is more pronounced in sulfuric acid solution. The peak marked (ii) in Fig. 7b at about 1560 cm^{-1}, which exhibits a Stark shift of about 100 cm^{-1} V^{-1}, is tentatively ascribed to adsorbed NO species (see Section 3). The weak band at about 1460 cm^{-1} in Fig. 7b was already discussed as probably due to bulk-like ammonium adsorbed in the OHP (see Section 3 to Fig. 6a and b). The appearance of the $NH_{3,ad}$ related peak (1280 cm^{-1}) at potentials around 0.4 V in the negative-going scan, accompanied by a decrease of the NO_{ad} related peak at 1560 cm^{-1}, suggests that the latter species are reduced and desorbed as ammonium when sweeping the electrode potential in neat acid (see Fig. 7b). Reductive desorption of adsorbed species resulting from ammonium adsorption has also been detected by differential electrochemical mass spectrometry (DEMS) in alkaline solution, where an increase in $m/z = 15$ signal was found at low potentials in the negative-going potential sweep after adsorption [31]. Furthermore, in acidic solutions reduction of adsorbed NO species was claimed to result in ammonium desorption [32].

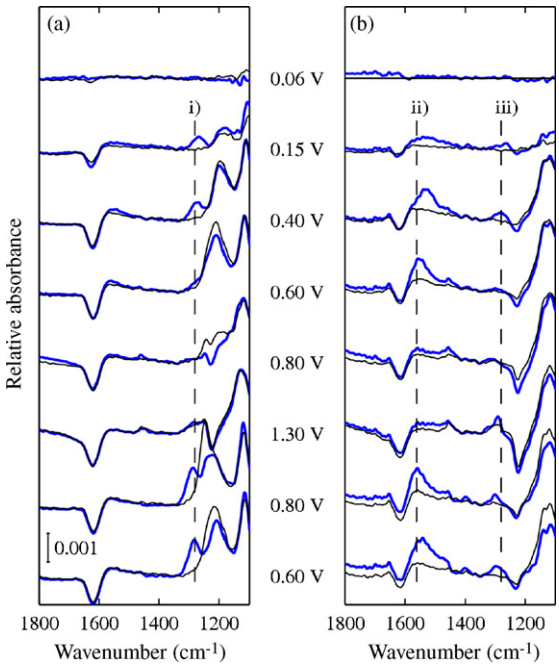

Fig. 7. Selected IR spectra from a set recorded during ammonium adsorbate stripping in neat, O_2-free acid after 5 min adsorption at 0.60 V in O_2-saturated (a) 0.50 M H_2SO_4 + 0.25 M NH_4OH or (b) 0.50 M $HClO_4$ + 0.25 M NH_4OH solution. The thick lines represent the spectra recorded in the first cycle (*i.e.*, from 0.60 → 1.30 → 0.06 V), thin lines denote the spectra observed in the following cycle (0.6 → 1.30 → 0.6 V). The reference spectrum was recorded in neat, O_2-free acid at 0.06 V, after adsorbate stripping. Assignment of bands: (i) and (iii) 'umbrella' mode of $NH_{3,ads}$, (ii) tentative assignment to NO_{ads}.

The bands at 1280, 1560 and 1460 cm^{-1} were observed during stripping, *i.e.*, in ammonium-free electrolyte, for adsorption potentials of 0.40 and 0.75 V as well, but not at 0.20 V (data not shown here). During adsorption (in ammonium-containing electrolyte), the NO_{ad}-related band at ~1560 cm^{-1} was found only in perchloric acid solution and only at 0.6 V, but not in sulfuric acid and not at other adsorption potentials used (0.20, 0.40, 0.75 and 1.10 V, spectra not shown). Finally, the bands at lower frequencies (one band in perchloric acid, Fig. 7b, and two bands in sulfuric acid, Fig. 7a) are due to adsorption of perchlorate and (bi-)sulfate and anions, respectively.

Combining the ORR results in Section 3.1 and the present IR results, the clear anion effect observed both for ORR activity and selectivity is probably due to co-adsorption of ammonia and (bi-)sulfate on Pt [25], which apparently reaches a higher total coverage than adsorption of ammonium alone, as is the case in perchloric acid solutions. The selectivity of the ORR is also influenced by these adsorbed species, in good agreement with results of previous studies on the effect of adsorbed anions (chloride) and CO adlayers on the selectivity of the ORR [12,17,18,21,22], showing that higher coverages of other adsorbates result in an increase in partial reduction of O_2 to form H_2O_2.

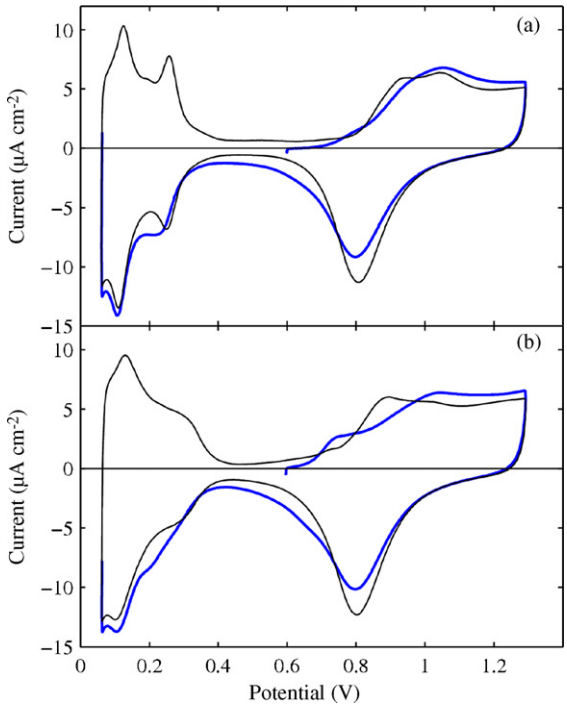

Fig. 8. Cyclic voltammograms recorded simultaneously with the IR spectra shown in Fig. 7 in neat O_2-free acid: (a) 0.50 M H_2SO_4 + 0.25 M NH_4OH and (b) 0.50 M $HClO_4$ + 0.25 M NH_4OH. The thick lines represent the first stripping cycle, the thinner lines show the following cycle.

CVs recorded simultaneously with the IR spectra during these adsorbate stripping experiments, after adsorption at 0.6 V in sulfuric acid solution (Fig. 8a) and in perchloric acid solution (Fig. 8b), respectively, are shown in Fig. 8. Again, both the first stripping cycle (thick line) and the second cycle (base voltammogram, thin line) are depicted. Reduction of the adsorbed residues clearly affects the Faradaic current in the stripping cycle, as evident from comparison with the subsequent base voltammogram (see also [19]). It is also noteworthy that no further effects of previous adsorption of ammonium could be noticed after the first cycle to low potentials, as the subsequent CVs fully coincide with CVs recorded in the base solutions in neat acid (not shown here).

In their characteristic features, the ammonium adsorbate stripping CVs shown in Fig. 8 largely resemble data obtained in bulk solutions of deaerated, ammonium-containing acidic solutions [19]. The most striking feature is that at least one adsorbate species, most likely an adsorbed nitric oxide species, can only be removed reductively at rather low potentials. The exact nature of this species, however, is still open. Similar results have also been observed for adsorbed NO species on Pt(1 0 0) [32] and for adsorbed ammonia on polycrystalline Pt in alkaline solutions [20,23]. We interpret this close similarity in such a way that an adsorbate which is different from the adsorbed NO species characterized by the 1560 cm^{-1} band, is formed in both perchloric acid and sulfuric acid solution at high potentials. This adsorbate is responsible for the increased H_2O_2 formation rate in the negative-going sweeps (see Figs. 1 and 3). In solutions with ammonium and sulfuric acid, these adsorbates also influence the ORR rate at potentials >0.5 V (see Fig. 5a).

The IR data help to understand the observation that in O_2-saturated bulk solutions the effect of ammonium is much more noticeable in the negative-going sweep than in the positive-going sweep both in perchloric and sulfuric acid solutions. In the negative-going scan the formation of hydrogen peroxide is much higher, at least down to potentials below 0.20–0.25 V, in the presence of ammonium in both perchloric and sulfuric acid solutions as compared to that in the neat acids (Figs. 1b and 3b). The IR spectra in Fig. 7a and b show that the bands related to adsorbed species originating from ammonium adsorption were present until the electrode potential was swept to potentials below ~0.15 V, where they could be reductively removed. In the subsequent sweep (spectra shown as thin lines in Fig. 7a and b), the bands due to ammonium adsorption were not present, and only those bands also seen in neat acid could be detected. At the same time, the formation of hydrogen peroxide was similarly low as that in the neat acids, showing that the species responsible for the change in ORR selectivity also have been removed at low potentials. Reductive removal of adsorbates is further supported by the CVs shown in Fig. 8, where the CVs measured after stripping of pre-adsorbed species were identical to those recorded in neat acids.

In potentiodynamic measurements in ammonium-containing, O_2-saturated perchloric and sulfuric acid solutions, the increased formation of hydrogen peroxide in the negative-going scans is clearly seen (Figs. 1b and 3b). The increased H_2O_2 formation rate closely resembles the higher H_2O_2 formation rate during adsorbate stripping in O_2-saturated neat electrolytes. In the positive-going scans, there was no effect of ammonium on the ORR selectivity in perchloric acid solutions (Fig. 1b), but in sulfuric acid solution the formation rate of hydrogen peroxide increased significantly in ammonium-containing solution compared to that in neat acid solution at potentials above 0.25 V (Fig. 3b). IR spectra recorded on Pt electrodes exposed to ammonium-containing solutions (not shown here) showed a band at 1280 cm^{-1} assigned to adsorbed ammonia ($NH_{3,ad}$). This adsorbate, however, has only an effect on the ORR selectivity in sulfuric acid solutions, not in perchloric acid solution, indicating that the presence of the adsorbed ammonia species is not sufficient to affect the ORR selectivity. Marked variations in the ORR selectivity, leading to increased H_2O_2 formation, are only obtained for coadsorption of ammonia and (bi-)sulfate species. In electrochemical quartz crystal microbalance measurements in ammonium-containing sulfuric acid electrolyte [19], the formation of adsorbed species was proposed to explain the hysteresis in the mass signal commencing at 0.30 V, which is not seen in neat acid. The present data confirm and extend this previous proposal: the increase in mass is related to ammonium adsorbate formation at elevated potentials (0.6–0.7 V) and coadsorption of (bi-)sulfate anions. These adsorbates are desorbed ((bi-)sulfate) or reductively removed (ammonium adsorbates) at significantly more cathodic potentials, indicative of a stabilizing interaction between these two adsorbed species. The formation of a pronounced hysteresis observed in Fig. 3b and, to a lesser extent, also in Fig. 1b, is also supported by the slow adsorption of ammonium (formation of ammonium adsorbate) even at elevated potentials, which is illustrated by the

adsorption transients in Fig. 4. This means, that the uptake of ammonium adsorbates continues also, after scan reversal, in the negative-going scan when reaching the active potential region at about 0.8 V, leading to much more pronounced effects on the ORR in the negative-going scan than in the positive-going scan.

4. Conclusions

In electrochemical and *in situ* ATR–FTIRS flow cell measurements with continuous controlled electrolyte transport the effect of ammonium on the ORR activity and selectivity on polycrystalline Pt electrodes was found to depend sensitively on the electrolyte and the reaction potential. The influence of ammonium on the ORR activity in perchloric acid solutions was little, while in sulfate solutions this was significant. Adsorbates formed at potentials above 0.40 V in solutions with ammonium and sulfuric acid are proposed to influence the ORR activity. An increased yield of hydrogen peroxide in the presence of ammonium was found, particularly in sulfuric acid solutions, but also in perchloric acid solutions. An increased H_2O_2 yield in sulfuric acid solution was observed at lower potentials than ammonium-related effects on the ORR activity in potentiodynamic measurements, suggesting that, if the same species is responsible for both activity and selectivity effects, the ORR selectivity is affected at lower coverage than the ORR activity. Alternatively, different species may be responsible for activity and selectivity effects. The formation of H_2O_2 was highest for adsorption potentials in the range from 0.6–0.7 V (potentiostatic measurements), but H_2O_2 formation was also observed at higher potentials (0.80–0.90 V), where fuel cell cathodes typically operate. This is important due to its possible impact on the long-term stability of fuel cells exposed to fuel gases and/or air containing ammonia. Adsorption transients show that ammonium-induced electrode poisoning is slow; no steady state was reached within 10 min. Adsorbed species, assigned to ammonium and nitric oxide, were detected on a Pt film electrode by *in situ* FTIRS. Adsorbed nitric oxide could only be observed in perchloric acid solutions, and is thus not likely to be responsible for the effect of ammonium on ORR activity and selectivity. Adsorbed ammonia was detected in the IR spectra in both electrolytes. In sulfuric acid solution, it is stabilized by coadsorption with (bi-)sulfate, forming an adsorbate with higher total coverage than in perchloric acid. This can explain the larger effect of ammonium on the ORR kinetics and selectivity in sulfuric acid compared to perchloric acid. Another adsorbed species, probably an adsorbed nitric oxide formed at higher potentials, influenced the selectivity of the ORR, in addition to oxidized platinum, in both perchloric and sulfuric acid in the negative-going scans so that more hydrogen peroxide was formed. At potentials below ~0.15 V, these adsorbates were quantitatively reductively removed in stripping experiments, and in subsequent positive-going scans the selectivity of the ORR was similar to that in neat acid solutions for both perchloric and sulfuric acid solutions. The exact nature of this adsorbed nitrogen oxide species was not identified.

Acknowledgement

The work supported by the Federal Ministry of Education and Research (BMBF) under contract 01 SF 0053.

References

[1] F.A. Uribe, S. Gottesfeld, T.A. Zawodzinski Jr., J. Electrochem. Soc. 149 (2002) A293–A296.
[2] H.J. Soto, W.-K. Lee, J.W. Van Zee, M. Murthy, Electrochem. Solid State Lett. 6 (2003) A133.
[3] R. Halseid, P.J.S. Vie, R. Tunold, J. Power Sources 154 (2006) 343.
[4] R. Borup, M. Inbody, J. Tafoya, T. Semelsberger, L. Perry, Durability Studies: Gasoline/Reformate Durability, http://www1.eere.energy.gov/hydrogenandfuelcells/pdfs/nn0123ba.pdf, 2002.
[5] H.-Y. Zhu, J. Alloys Compd. 240 (1996) L1.
[6] R. Halseid, P.J.S. Vie, R. Tunold, J. Electrochem. Soc. 151 (2004) A381.
[7] R. Halseid, T. Bystron, R. Tunold, Electrochim. Acta 51 (2006) 2737.
[8] S.T. Szymanski, G.A. Gruver, M. Katz, H.R. Kunz, J. Electrochem. Soc. 127 (2006) 1440.
[9] D.E. Curtin, R.D. Lousenberg, T.J. Henry, P.C. Tangemann, M.E. Tisack, J. Power Sources 131 (2004) 41.
[10] V.O. Mittal, H.R. Kunz, J.M. Fenton, Electrochem. Solid State Lett. 9 (2006) A299.
[11] Z. Jusys, J. Kaiser, R.J. Behm, Electrochim. Acta 49 (2004) 1297.
[12] U.A. Paulus, T.J. Schmidt, H.A. Gasteiger, R.J. Behm, J. Electrochem. Soc. 495 (2001) 134.
[13] T. Biegler, D.A.J. Rand, R. Woods, J. Electroanal. Chem. 29 (1971) 269.
[14] M. Osawa, K. Ataka, K. Yoshi, T. Yotsuyanagi, J. Electron. Spectrosc. Rel. Phenom. 64–65 (1993) 371.
[15] Y.-X. Chen, M. Heinen, Z. Jusys, R.J. Behm, Angew. Chem. Int. Ed. 45 (2006) 981.
[16] A. Miki, S. Ye, M. Osawa, Chem. Commun. (2002) 1500.
[17] T.J. Schmidt, U.A. Paulus, H.A. Gasteiger, R.J. Behm, J. Electroanal. Chem. 508 (2001) 41.
[18] Z. Jusys, J. Kaiser, R.J. Behm, J. Phys. Chem. B 108 (2004) 7893.
[19] R. Halseid, J.S. Wainright, R.F. Savinell, R. Tunold, J. Electrochem. Soc. 154 (2007) B263.
[20] A.C.A. de Vooys, M.T.M. Koper, R.A. van Santen, J.A.R. Van Veen, J. Electroanal. Chem. 506 (2001) 127.
[21] U.A. Paulus, T.J. Schmidt, H.A. Gasteiger, in: W. Vielstich, H.A. Gasteiger, A. Lamm (Eds.), Electrocatalysis, vol. 2, Wiley, Chichester, 2003.
[22] V. Stamenkovic, B.N. Grgur, P.N. Ross, N.M. Markovic, J. Electrochem. Soc. 152 (2005) A277.
[23] J.K. Wang, N.M. Markovic, R.R. Adzic, J. Phys. Chem. B 108 (2004) 4127.
[24] R. Halseid, PhD Thesis, Norwegian University of Science and Technology, 2004.
[25] Y. Shingaya, H. Kubo, M. Ito, Surf. Sci. 427–428 (1999) 173.
[26] D.S. Corrigan, M.J. Weaver, J. Electroanal. Chem. 239 (1988) 55.
[27] V. Rosca, G.L. Beltramo, M.T.M. Koper, Langmuir 21 (2005) 1448.
[28] M.J. Weaver, S. Zou, C. Tang, J. Chem. Phys. 111 (1999) 368.
[29] R. Gómez, A. Rodes, J.M. Orts, J.M. Feliu, J.M. Pérez, Surf. Sci. 342 (1995) L1104.
[30] K. Momoi, M.B. Song, M. Ito, J. Electroanal. Chem. 473 (1999) 43.
[31] S. Wasmus, E.J. Vasini, M. Krausa, H.T. Mishima, W. Vielstich, Electrochim. Acta 39 (1994) 23.
[32] V. Rosca, M.T.M. Koper, J. Phys. Chem. B 109 (2005) 16750.